

## RESEARCH ARTICLE

# Development and Characterization of a Directional Gamma-ray Detector

Felix Cormier<sup>1</sup>, Marcel Georgin<sup>1\*</sup>, Stephen Koelbl<sup>2</sup>, Robert Oda<sup>3</sup>

<sup>1</sup>Department of Physics, McGill University, Montreal, QC, Canada

<sup>2</sup>Department of Physics and Department of Physiology, McGill University, Montreal, QC, Canada

<sup>3</sup>Department of Physics and School of Computer Science, McGill University, Montreal, QC, Canada

\*Email Correspondence:  
marcel.georgin@mail.mcgill.ca

### Keywords

High Energy Physics

Gamma Ray Detection

Directional Detector

Applied Physics

Silicon Photomultipliers

## Abstract

**Background:** This work characterizes the first generation of detectors from the Hanna Laboratory to implement Silicon Photomultipliers and a heptagonal scintillator conformation. The purpose of the device is to determine the angle at which a radioactive source is located.

**Methods:** The development of the detector consisted of three phases: construction (September 2012–December 2012), simulation and characterization (April 2013). The experimental portion of the work consisted of placing a  $^{137}\text{Cs}$  source at an arbitrary location, measuring the count rates in each scintillator panel and analysing the results.

**Results:** The detector's function was validated by confirming the inverse square law with a radioactive source moving away from the detector. Furthermore, with a  $\chi^2$  summation method of analysis the angular position of a source was determined with an accuracy of  $10^\circ$  and a precision of  $12^\circ$ . With a normalisation method of analysis the angular position of a source was found with an accuracy of  $2^\circ$  and a corresponding precision of  $2^\circ$ .

**Limitations:** The quality of the electronics handling the signal from the silicon photomultipliers limited our resolution. Occasional double counts occur when a large amount of energy is imparted to the scintillator. Furthermore, the custom-built circuitry lowered the signal-to-noise ratio such that large distances were not feasible due to electronic noise constraints. Finally, simulation data analysis showed that the break of one circuit only had a small effect on the  $\chi^2$  method of analysis.

**Conclusions:** In conclusion, the design of the detector and the analysis techniques were shown to be suitable for short range angular resolution of a gamma-ray source. Both distance trials and a simulation of the detector prototype confirmed the validity of our design and of the analysis methods used. These promising results at short distances motivate further work in electronic circuit design to improve the range while maintaining both accuracy and precision.

## Introduction

### Motivation

The inspiration for the development of a scintillating directional gamma-ray detector is the BATSE (Burst And Transient Source Experiment), an experiment on the National Aeronautics and Space Administration's (NASA) Compton Gamma Ray Observatory Satellite looking for gamma-ray bursts (1). A scintillating detector is made of material that will release photons when struck with radiation - these

photons can then be picked up by specific electronics. The BATSE experiment used eight scintillating modules to determine the direction of a gamma ray source in space. These modules were made of two scintillating components. Thallium doped Sodium Iodide was the first scintillating material used and it allowed the observatory to detect gamma-rays within an energy range of 20 keV to 2 MeV. The second component was made of pure Sodium Iodide, which extended the modules energy range to approximately 8 MeV allowing the experiment to detect more powerful sources. This device was ultimately used to detect cosmic gamma-ray sources by relying on the

fact that scintillators which had a greater effective area (thus facing the source) would have a greater count rate (1).

Luc Sagnière from the Hanna Laboratory developed an octagonal (eight sided) Gamma-ray Detector (OGD) using this proven platform. The purpose of this device was to quickly detect the angular position of a terrestrial gamma-ray source rather than detection of gamma ray sources in space. This was accomplished by orienting eight scintillating plates in an octagon and using photo-multipliers to collect and convert the light into a current, which could be converted to a count rate. The count rate in each of the eight channels is then analysed to determine the angular position of the radiation source (2).

The current iteration of the directional gamma-ray detector prototype takes advantage of developments in both the geometry and the technology; rather than using an octagonal design and photo-multipliers of the OGD, a heptagonal (seven sided) geometry and silicon photo-multipliers were chosen to create the new Heptagonal Gamma-ray Detector (HGD).

## Design

Previously, the OGD difficulties determining the origin of a radiation source because of the symmetry in the octagonal shape. Due to the bilateral symmetry in the previous design, both the nearest and farthest faces would have high count rates, creating an ambiguity in the results. This is shown in the right hand side of Fig. 1.

To solve this problem, the design of the detector takes advantage of the change in the solid angle of each face with which the gamma radiation can interact. The closest face normal to the incident radiation will have the greatest cross sectional area and therefore the most interaction with the gamma rays. The faces which are at steeper angles will have a significantly reduced effective area of interaction. This reduction in solid angle is shown clearly in Fig. 1(a). The cross sectional area in (1) from Fig. 1(a) is much greater than that of (2).

During experimental setup and calibration, the circuit connected to one of the scintillators was damaged. Several attempts to repair were made however it was not possible to complete these repairs within the allocated time frame of the project. The project was completed with the remaining six faces.

## Polyvinyl Toluene

Scintillators are materials that convert short-wavelength photons, such as gamma-rays, into longer wavelength photons. This is accomplished via a process called Compton scattering where a gamma ray inelastically collides with an atomic electron and deposits energy. This excited electron then re-emits a longer wavelength photon through either fluorescence or phosphorescence. These emitted photons are contained in the scintillator until detected by an at-

tached photomultiplier. Polyvinyltoluene (PVT) is an organic plastic scintillator which emits light at a wavelength of 423 nm (3). PVT was selected as the scintillating material because of its rapid decay time of 2.4ns. Furthermore, it is transparent to its own emissions - this is very important as opacity would result in signal loss. Beyond its physical properties, an additional reason for the selector of PVT was the low cost of the material (4).

## Silicon Photomultiplier & Circuit

Silicon Photomultipliers (SiPMs) are the semiconductor analog to the traditional photomultiplier tube. Silicon photo-multipliers are built from an array of avalanche photodiodes on a common silicon substrate. An avalanche photodiode (APD) is a device which takes advantage of the photoelectric effect to generate a current from the impact of a photon at the p-n junction. A bias voltage generates an electric field at the interface between the n and p type silicon semiconductor. The field is so large ( $\approx 5 \times 10^3$  V/cm) that a single photon interaction with the pixel can produce a large enough cascade of electrons to generate a detectable current (5).

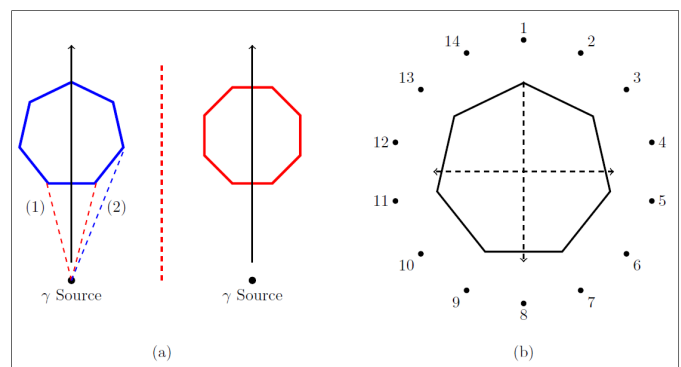


**Fig. 1**

**(a)** Basic geometry of the detector. The theory is that the change in the solid angle between (1) and (2) will cause a change in the count rate. Degenerate results were due to scintillators being parallel in the octagonal geometry of the detector (red). This was avoided by using the seven sided geometry on the left.

**(b)** Plan of the detector with 14 calibration points labeled around the panels. This diagram is the basis for the entire calculation of the angle. All angles will be referred to from angle 1 set as  $\theta = 0$ .

For the development of the HGD, the ArraySM-4 silicon photomultiplier from SensL was implemented as the converter of optical photons into a current. This SiPM's peak absorption wavelength is at 500nm and it has an internal gain of  $2.3 \times 10^6$  per pixel; the scintillator material, polyvinyl toluene, outputs green photons to match the 500nm absorption wavelength. In total, the ArraySM-4 has sixteen pixels each with their own output. A silicon photomultiplier was chosen over a photomultiplier tube for several reasons: it is more compact and has lower bias voltage requirements. The readout electronics used in the gamma ray detector were custom-built to operate with the SiPM as part of this project (6). This SiPM was biased by a custom designed circuit. Additionally, this same circuit was used to amplify the signal from the SiPM and transfer it to the data acquisition system described in Section 3.2.

## Methods

### Experimental Setup

Each PVT face is made of a 25 cm tall by 7.5 cm wide by 2 cm thick piece of PVT plastic scintillator. Each scintillator was wrapped in Tyvek to improve the internal reflectivity and then wrapped again with electrical tape to isolate the face from the ambient light. At the top of the each face, a hole was cut out in the protective wrapping to place the SiPM in contact with the PVT. The SiPM is then interfaced with its own amplifying circuit, described in Section 2.4, and then rewrapped to ensure that the system was light tight. The circuit then sends the signal to the data acquisition system. This was repeated for each individual scintillator, meaning there were seven scintillators, SiPMs and amplifying circuits.

### Data Acquisition System

The data acquisition process was identical for each of the six active faces of the HGD. First the signal from the amplifying circuit was passed into a discriminator whose threshold is determined by the calibration in Section 3.4. This discriminator outputs a NIM pulse (-0.7 V) for every input pulse at greater voltage amplitude than the threshold. This signal was then passed to a scaler which counts the number of NIM pulses for each circuit. The duration of each trial and the number of trials is determined by the user through programming of a CAMAC module using C++. The CAMAC data acquisition system serves as the conversion program between NIM pulses and digital output to be analysed.

### Simulation

In parallel to the construction of the detector, a simulation was created to virtually run experiments using the Geant4 system. This system was developed to simulate high energy particle physics experimentation. Written in C++, the simulation utilized Monte Carlo methods

to test the detector's geometry and detection by allowing users to construct a virtual model of an experiment and programming the behavior of various types of radioactive sources (7).

One of the circuits was damaged during testing. This simulation proved to be vital to the experiment as it modelled a full working set of panels; this allowed for full calibration of the virtual system and a full set of data to compare results with the physical detector.

### Calibration

The first step in calibrating the detector is setting the gain of the individual photomultiplier circuits as well as the threshold of the discriminator connected to the circuit's output. The gain is the amplitude of the voltage response to a gamma ray. This was first determined by minimizing the signal to noise ratio. Then, a threshold curve was made to calibrate the discriminator threshold for each circuit.

#### Gain

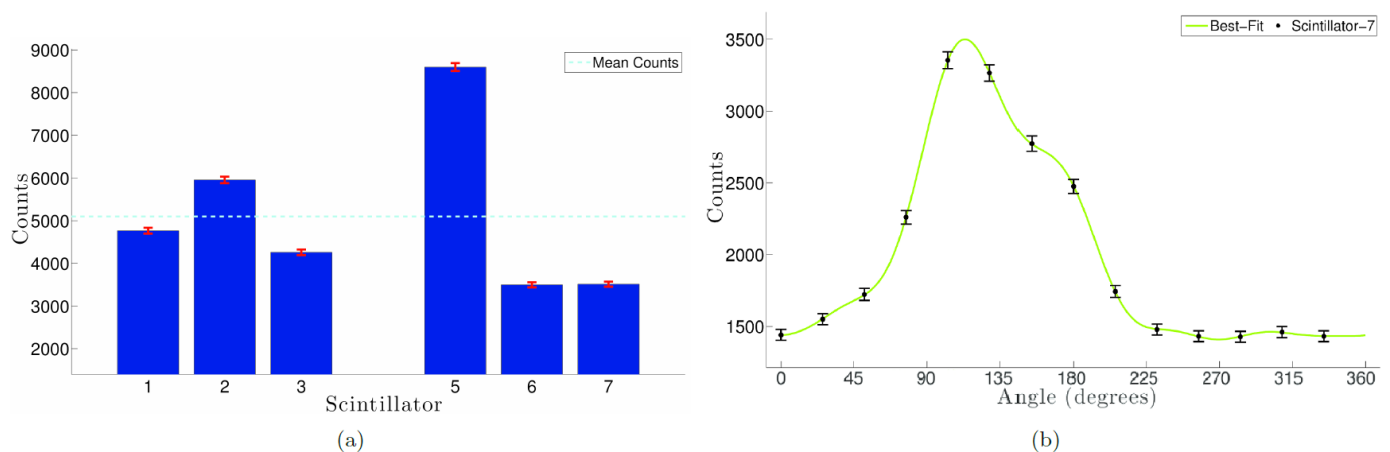
The gain set for each individual circuit was chosen such that two different parameters were satisfied. First, the voltage response for each scintillator to a gamma ray had to be equal for each circuit, within uncertainty. Second, the electronic noise in the output had to be less than 10% of the gamma ray voltage. Since the gain was determined by a potentiometer, there was no absolute gain measurement, however, the circuits could be compared to equalize their relative gains.

The instrument used for measurement was an oscilloscope. By viewing the circuit output with and without a radioactive source, the gamma ray voltage output and the electronic noise could be compared. This could be done using the oscilloscope digital tools which measured maximum and mean voltage.

To begin the calibration, the gain of the circuit with the lowest signal-to-noise ratio was set to have its noise be about 10% of its gamma ray voltage. Quantitatively, for a  $^{137}\text{Cs}$  source, this equates to a voltage response of 0.68(3) V for a gamma ray, and 0.07(3) V for the electronic noise. Then, the gain of the other circuits was adjusted such that a gamma ray from a  $^{137}\text{Cs}$  source would output a voltage of 0.68 V, within one standard deviation.

#### Threshold

With the gain set, a threshold curve was constructed for every circuit. This was done by incrementally decreasing the discriminator threshold and measuring the count rate. For every channel, the count rate stayed about constant until a certain threshold value was reached, then the count rate started exponentially increasing. The threshold value about 50mV before this exponential increase was chosen for every channel, so as to stay below the noise. Threshold for every channel was very similar, with values around the 200 mV range.

**Fig. 2**

**(a)** Calibration data for the normalization analysis method. **(b)** Calibration data for the 2 summation analysis method. This figure shows the number of counts for scintillator 7; every data point is one of the calibration angles. It is fit with a 6-term Fourier series with a period of 360.

### Angle Calibration

The final step in calibrating the detector is placing the  $^{137}\text{Cs}$  source at all the points shown on Fig. 1(b). For every point, count rates are measured for every scintillator. This gives a baseline set of data to compare to when a radioactive source is placed at a random angle. All angles will be referred to from angle 1 from Fig. 1(b) as  $\theta = 0$  rad.

This calibration procedure will output a graph such as Fig. 2b for every scintillator. By comparing results for calibration points and random points for every scintillator, a  $\chi^2$  method of analysis can be used to reconstruct the random angle. Similarly, using Fig. 2a, counts can be normalized for every scintillator, and used as part of the normalization analysis method.

### Distance Sensitivity

The distance sensitivity was tested by placing a radioactive source directly in front of one of the scintillators and displacing the source away from this scintillator perpendicularly to its surface. This test is designed to verify the well known  $\frac{1}{r^2}$  relationship between the position of the source with respect to the detector and the intensity of the radiation at the detector. This test was completed by placing the source in front of scintillator 1 and moving it radially outward in intervals of 8.0(2) cm to a maximum of 64.0(2) cm. It will also determine the effective range of the detector; information which can be used to setup further testing as in Section 3.6.

### Angular Resolution

A subsequent experiment was conducted. To do this, three random angles were chosen ( $63^\circ(2)$ ,  $117^\circ(2)$  and  $299^\circ(2)$ ). Using the results from the distance sensitivity trial, a distance where the scintillators

counts are well above the noise was chosen. Two methods to resolve the position of the radioactive source were developed: the  $\chi^2$  method and the normalisation method. Both methods were used to determine the location of a randomly positioned source. Two of the angles were also analysed in the simulation to provide a quantitative comparison.

## Results

### Validation of the Inverse Square Law

By changing the distance of the source with respect to one of the scintillators, the sensitivity of the detector to changes in source position can be determined. Fig. 3 shows the result of the distance test which used a  $\chi^2$  minimization method to fit the data acquired. The equation obtained for scintillator 1 is shown in Equation (1).

$$y = \frac{9.1 \times 10^5}{(x + 5.1)^2} + 9.4 \times 10^2 \quad (1)$$

In this case, the inverse square law can be confirmed if it can be shown that the fit is of statistical significance. To do this, the p-value of this fit is computed, giving a value of 0.999 from which it can be concluded that the data fits an inverse square law. Finally, a distance between 10 and 15 cm was used for the random source test as these are well above the noise pedestal encountered at around 60 cm.

### Angular Resolution

#### $\chi^2$ Method of Source Location

The first step in the  $\chi^2$  method is obtaining the calibration data from the 14 points on Fig. 1(b) and fitting the data using a six-term Fourier series, as seen in Fig. 2b. This is done for each scintillator. The use of

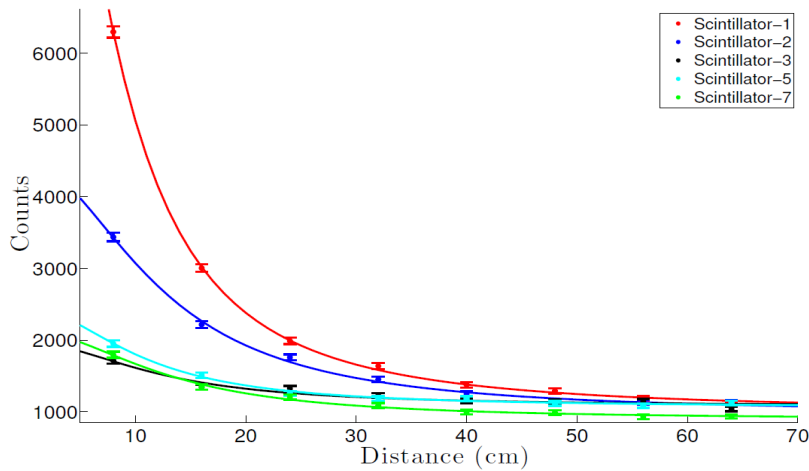


**Fig. 3**  
The number of counts for each of the 7 scintillators as the source is moved outwardly away from the detector. The source was placed at position 1 ( Fig. 1(b)). As can be seen, the best-fits follow the  $\frac{1}{r^2}$  relation, as expected.

a six term Fourier series was motivated by the work done by Luc Sagniere (2), who uses a six-term Fourier series, as well as the requirement that the fit be periodic over  $360^\circ$ . Then the Fourier series for each scintillator is compared to the data obtained at the random point using Equation (2).

$$\chi^2 = \frac{(y_i - y_i(\theta))^2}{\alpha_i^2} \quad (2)$$

In Equation (2)  $y_i$  is the number of counts registered by scintillator  $i$  when the radioactive source is placed at a random point, and is thus a constant for each scintillator.  $y_i(\theta)$  is the number of counts predicted by the Fourier series fit for scintillator  $i$  as a function of angle done during calibration as explained in the previous paragraph, and  $\alpha_i$  is the error in the counts registered by scintillator  $i$ . The  $\chi^2$  function for each scintillator is calculated, then all these functions are added together to give the plots seen in Fig. 5. Note that the  $\chi^2$  is a function of  $\theta$ . The value of  $\theta$  for which the total  $\chi^2$  is smallest is the location of the source determined by the HGD.

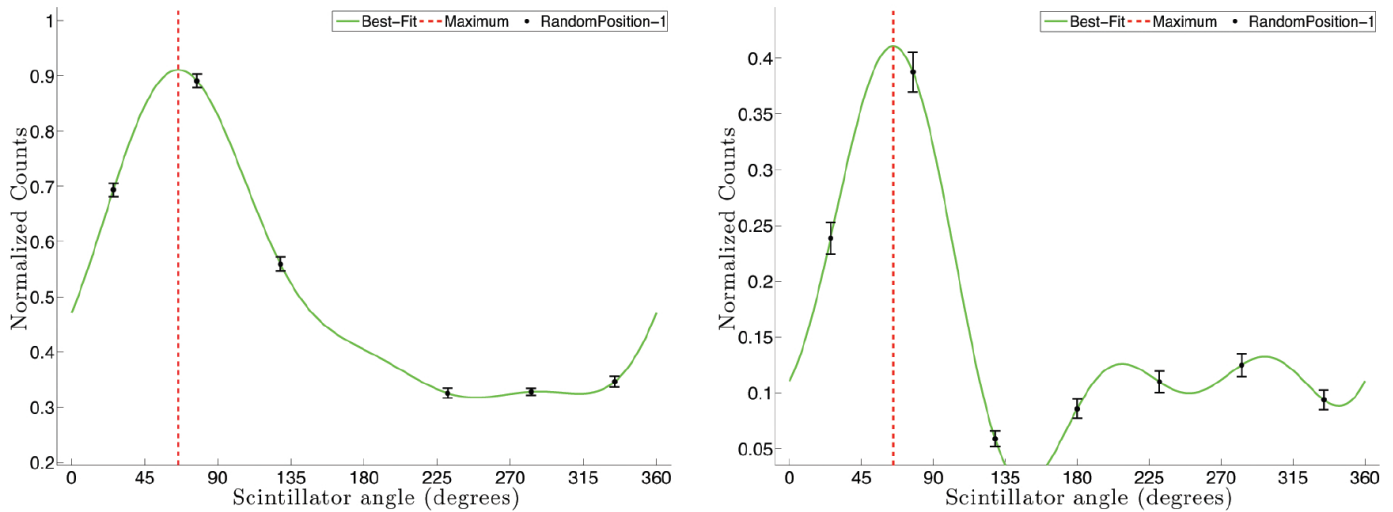
To obtain the uncertainty in the  $\chi^2$  analysis, error was propagated through by changing  $y$  in Equation (2) by  $\pm\alpha$ , then recomputing  $\chi^2$ , giving  $\chi^2_{upper}$  and  $\chi^2_{lower}$  respectively. The error in the measurement was found by locating the angles,  $\theta_{upper}$  and  $\theta_{lower}$  which correspond to minima in  $\chi^2_{upper}$  and  $\chi^2_{lower}$ . Computing  $\alpha_{upper} = \theta_{upper} - \theta$  and  $\alpha_{lower} = \theta - \theta_{lower}$  gives the error in the measurement. This type of non-traditional error analysis is important as this detector has been designed for on-the-fly angular measurements - this method thus allows for *in situ* angle and precision measurements.

Fig. 5 is the result of the  $\chi^2$  analysis for both the simulated and experimental data. A qualitative comparison between the simulated and experimental data shows that the performance of the HGD is

similar to what was expected from the simulation. Results for both simulation and experimental data for the random points are shown in Table 1. Quantitative differences between experimental and simulation data will be discussed in Section 5.4. For random position 1, the radioactive source was placed at  $63^\circ(2)$  with respect to angle 1 in Fig. 1(b). The experimental results from the  $\chi^2$  analysis method resolved the angular position of the source to be  $72^\circ(1)$ . Equivalent analysis of the simulated data computed the angular position of the source to be  $61.9^\circ(4)$ . Results for other positions are summarised in the above-mentioned table.

	Position Angle			
	Method	Random Point 1 (deg)	Random Point 2 (deg)	Random Point 3 (deg)
Real	$\chi^2$ Summation	72 (1)	291.4 (4)	105 (1)
	Normalization	65 (2)	290 (2)	122 (2)
Simulation	$\chi^2$ Summation	61.9 (4)	300.6 (4)	NA
	Normalization	64 (2)	293 (2)	NA
True Value		63 (2)	299 (2)	117 (2)

**Table 1**  
A summary of the calculated position angle of the random points. The method of finding the errors of these are discussed in detail in Section 4 and Section 5.



**Fig. 4**

After calibration, the normalised number of counts for random position 1 is shown for the real (left sub-figure) and simulated (right) data. A best-fit curve was found using a Fourier-6 (solid green line) is shown. The global maximum of the curve corresponds to the angle position of the source at random position 1.

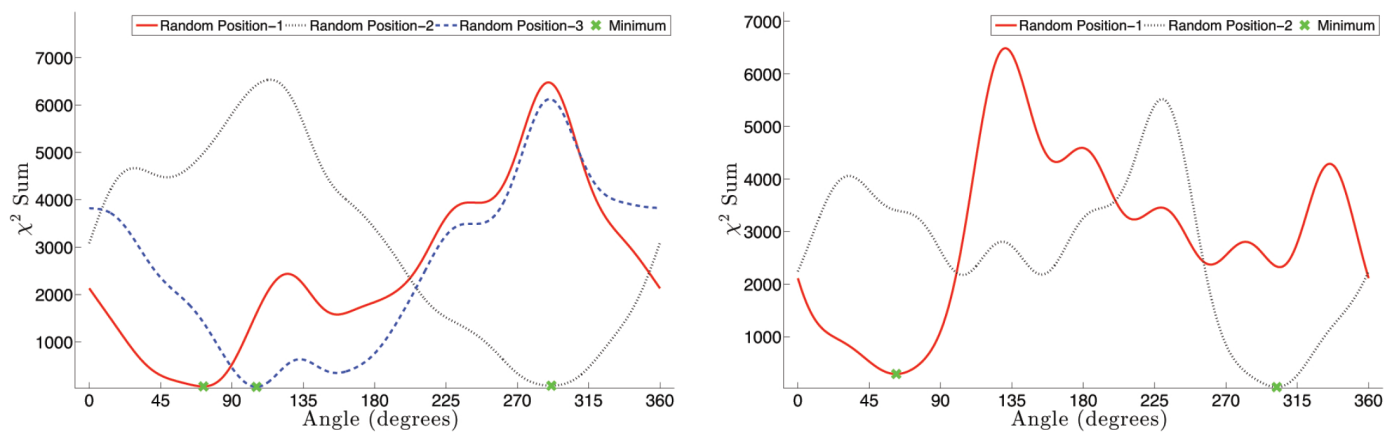


**Fig. 5**

For the experimental (left sub-figure) and simulated (right) data, the  $\chi^2$  summation for each of the random points are shown. The minimum for each  $\chi^2$  summation (green x) corresponds to the respective angle position of each random point. The determined angle position for the real and simulated data are comparable.

Normalisation Method of Source Location

The normalisation method uses the calibration points, seen in Fig. 2a, as normalisation factors for the data retrieved from the random position tests. The normalised counts in each scintillator are then fit with a six term Fourier series. The scintillator angle of the fit’s maximum is the location of the source. Fig. 4 shows a comparison between the results of the simulation and the HGD. This qualitative comparison shows that the signal quality of the detector is what was expected from the Geant4 simulation.

For the normalization method, the error on the fitting parameters was negligible. Thus, the error on the normalization counts, as shown in Fig. 2a, was used. Since this was a counting experiment, the square root of the counts was used as the error, propagated through the normalization analysis method, and output as a 2° uncertainty. This again allows for an in-situ analysis of the angle, as in the  $\chi^2$  analysis method.

Results for both experimental and simulated data are shown in

Table 1. For random angle 1, where the radioactive source was placed at  $63^\circ(2)$ , the experimental results from the normalisation analysis method calculated the angular position of the source to be  $65^\circ(2)$ . In parallel, analysis of the simulated data computed the angular position of the source to be  $65^\circ(2)$ . The rest of the results are summarised in the above-mentioned table.

## Discussion

The primary objective of this research was to demonstrate a proof of concept for a heptagonal gamma-ray detector design. To achieve this goal, a simulation as well as a two part experiment was conducted. The goal of the simulation was to first validate the design of the detector and subsequently act as reference for comparison to future experiments. Because one of the detector faces was damaged, the simulation allowed us to see the effect of the loss of a circuit. Table 1 shows that the  $\chi^2$  summation analysis method was consistently less accurate *in situ* than in the simulation while the normalisation method was not affected as much by the loss of a face. The first experiment tested the radial sensitivity of the detector. Beyond testing the ability of the HGD to resolve sources at a distance, this test was designed to observe the  $\frac{1}{r^2}$  law as a verification of the detector's circuitry. The second experiment tested the ability of the HGD to resolve the angular position of a source. In conjunction, these tests were able to show that the HGD was a successful initial prototype. Table 1 summarizes all the results obtained from both the  $\chi^2$  and normalisation methods.

### Analysing the Relationship Between Distance and Counts

By varying the of distance between a radiation source and the detector, we were able to draw several conclusions about the performance of the detector. The inverse square law for distance served as a verification of the circuit design and data acquisition methods.

Finally, the distance sensitivity shows that at around the maximum distance studied, 64 cm, the derivative approaches 0 as the data obtained becomes dominated by the noise. This leads to the conclusion that the maximum distance for which the detector could resolve the position of a radioactive source that had the same output as the radioactive sample used, is 64 cm. This restriction is due to the gain of the individual scintillator's circuits. Each circuit had a threshold as well as background noise which created counts not from the radioactive source studied this could be natural radiation like cosmic rays or natural sources in the surroundings. Efforts were made to increase the signal-to-noise ratio which led to the results shown in Section 5.1. With a refinement in the electronics used to shape the signal from each scintillator, it is very likely that a future iteration of this project could succeed at distances much larger than those seen here.

## Qualitative Analysis

A qualitative comparison of the experimental and simulated results can now be made. In Fig. 4 (experimental on the left, simulated on the right), we see that the shape of the data and best fit curves are similar. The simulated data represents the number of times energy was deposited in a scintillator face. Therefore, the correlation between the shapes in Fig. 4 suggests that the SiPM in the electronics is correctly collecting the light from the scintillator in proportion to the number of incident gamma-rays.

## Analysis methods

The two analysis methods used,  $\chi^2$  and normalisation, were both successful at determining the angle of the radioactive source with respect to the detector. In terms of the results shown in their respective sections, the  $\chi^2$  method analysed the position to be 8 times the uncertainty in the measurement from the actual position for the experimental results and 3 times the uncertainty in the measurement for the simulation. For the normalisation method, the experimental and simulated results were both only 1 times the uncertainty in the measurement from the actual value. For every position attempted, the results determined from normalisation analysis were more accurate and precise than those determined through the  $\chi^2$  method of analysis.

Thus using the normalisation method of analysis gives an excellent approximation of the angle of the source with respect to the detector, and shows the success of the heptagonal detector at low distances.

## Error Sources and Improvements

Several factors during the construction and testing of the device negatively affected the performance of the HGD.

The use of SiPM's reduced the size and weight of the device compared to previous models, however, during long tests, the gain within the device was found to vary significantly with time and possibly also with temperature. This led to difficulty in calibration and ultimately device performance.

During the construction of the HGD, there was a design change in the amplifying circuit in which the old circuit boards were modified for a new, simplified design. Using this make-shift circuitry likely induced a significant amount of noise in the signal received from the SiPMs. The circuit used in testing also caused ringing in the pulse which occasionally resulted in double counts in the scaler. Using a new circuit board would likely significantly improve the signal to noise ratio and ultimately the performance.

The loss of the amplifying circuit from the seventh face of the detec-

tor during testing likely affected performance, however this cannot be known as the circuit could not be fixed. The results of the tests show that the detector was still able to perform despite the missing face which suggests robustness to failure in the design of the HGD.

The HGD's ability to detect a source at a distance was worse than expected. This was mostly due to the signal to noise ratio. With a  $0.1 \mu\text{C } ^{137}\text{Cs}$  source, the signal from the HGD was reduced to noise levels after the source was moved 64 cm away from the detector.

Considering these aforementioned problems in the development of the HGD, the detector still qualitatively performed as predicted by the Geant4 simulation. The detector was capable of determining the location of a source accurately. Even though the distance away from the detector was small, this is still a successful proof of concept and with some modifications could provide the performance required to detect more distance sources.

## Conclusion

In conclusion, the design of the detector and the analysis techniques were shown to be suitable for short range angular resolution of a gamma-ray source. Both distance trials and a simulation of the detector prototype confirmed the validity of our design and of the analysis methods used. Using normalisation analysis at small distances, the detector was accurate within  $2^\circ$  of its true angular position. The uncertainty of the position calculation was  $2^\circ$ . These promising results at short distances motivate further work in electronic circuit design to improve the range while maintaining both accuracy and precision to within the values outlined in this report.

## Acknowledgements

We would like to thank Professor David Hanna for allowing us to use his laboratory and his equipment for the construction and testing of the detector, Audrey MacLeod for her help with understanding the physics behind the detector, Adam Gilbert for assistance with the circuit design and testing, and Sean Griffin for help with programming the control code for the CAMAC module.

## References

- [1] Meegan, C , Fishman, G , Wilson, R , Brock, M , Horack, J, Paciasas, W , Kouveliotou, C . The spatial distribution of gamma-ray bursts observed by BATSE. In: AIP Conference Proceedings. vol. 265; p. 61.
- [2] Sangiere L. A Gamma-Ray Directional Detector; 2012.
- [3] Birks JB. Energy transfer in organic systems VI. Fluorescence response functions and scintillation pulse shapes. *Journal of Physics B: Atomic and Molecular Physics*. 1968;1(5):946. Available from: <http://stacks.iop.org/0022-3700/1/i=5/a=323>.
- [4] Rakes KD. Evaluating The Response Of Polyvinyl Toluene Scintillators Used In Portal Detectors. Air Force Institute of Technology Wright-Patterson; 2008.
- [5] Buzhan. An Advanced Study of Silicon Photomultiplier; 2003.
- [6] Silicon Photomultipliers by SensL; 2013.
- [7] Agostinelli S, Allison J, Amako K, Apostolakis J, Araujo H, Arce P, et al. Geant4a simulation toolkit. *Nuclear Instruments and Methods in Physics Research Section A: Accelerators, Spectrometers, Detectors and Associated Equipment*. 2003;506(3):250 { 303. Available from: <http://www.sciencedirect.com/science/article/pii/S0168900203013688>.